9-2016

Copper(I) Thiocyanate Networks with Aliphatic Sulfide Ligands

Gerardo Ayala

Robert D. Pike
William & Mary, rdpike@wm.edu

Recommended Citation

Ayala, Gerardo and Pike, Robert D., Copper(I) Thiocyanate Networks with Aliphatic Sulfide Ligands (2016). *Polyhedron*, 115, 242-246.
https://doi.org/10.1016/j.poly.2016.05.029

Polyhedron 115 (2016) 242–246

Contents lists available at ScienceDirect

Polyhedron

journal homepage: www.elsevier.com/locate/poly

Copper(I) thiocyanate networks with aliphatic sulfide ligands

Gerardo Ayala, Robert D. Pike *

Department of Chemistry, College of William and Mary, Williamsburg, VA 23187, United States

ARTICLE INFO

Article history:
Received 12 March 2016
Accepted 12 May 2016
Available online 18 May 2016

Keywords:
Copper thiocyanate complexes
Crystal structures
Sulfide ligands
Network structures
Thermogravimetry

ABSTRACT

A total of five new CuSCN-L compounds with alkyl sulfide ligands, L = methyl sulfide (Me_2S), ethyl sulfide (Et_2S), isopropyl sulfide ($Pr^i{}_2S$) or tetrahydrothiophene (THT) have been prepared and characterized. X-ray crystal structures for four of the compounds were obtained. Two compounds were collected from solutions of CuSCN in Me_2S: $\{[Cu(SCN)(Me_2S)_2]\}_n$ (**1a**) in the form of colorless blocks and $(CuSCN)(Me_2S)$ (**1b**) as a white powder. Neat mixtures of CuSCN in the other alkyl sulfide ligands yielded only one product each: $\{[Cu(SCN)(Et_2S)]\}_n$ (**2**); $\{[Cu(SCN)(Pr^i{}_2S)]\}_n$ (**3**); and $\{[Cu(SCN)(THT)_2]\}_n$ (**4**). Crystals of **2** and **4** underwent destructive phase changes at lower temperatures. Two networks types were observed: 1:2 decorated 1-D chains (**1a** and **4**) and 1:2 decorated 1-D ladders (**2** and **3**). Further network formation through bridging of the organic sulfide ligands was not observed.

1. Introduction

Organosulfur ligands occupy an important niche in transition metal chemistry. As soft ligands, they are able to stabilize soft metal ions in low oxidation states. By virtue of their vacant d-orbitals and ancillary lone pairs, such ligands can potentially act either as π-donors or π-acceptors, depending upon their substituent electron demand. Sulfur ligands readily bridge metal centers, facilitating the formation of oligomers and polymers. Nevertheless, they also tend to solubilize metal salts, in particular Cu(I) salts. Thus, $CuX{\cdot}Me_2S$ (X = Cl, Br, I, and CN) is a convenient carrier of copper (I) salts in organic reactions [1]. There are many known complexes of CuX with sulfur ligands, including sulfides [2], thiolates [3], thioamides [4], and phosphine sulfides [5]. Their structural types include polymers and networks based on Cu_2X_2 dimers, Cu_2X_2 ladders, and $(CuX)_\infty$ polymers and oligomers. In some cases, such as that of CuI with tetrahydrothiophene (THT), many stoichiometries can be realized from the same combination of components [2f].

In the preceding paper, we described new networks of copper(I) thiocyanate coordinated with aromatic diimine ligands [6]. These fall into categories including 4-coordinate Cu and 3-coordinate Cu $(CuSCN)_\infty$ chains, $[Cu_2S(SCN)_2]_\infty$ ladders, and $(CuSCN)_\infty$ sheets. Surprisingly, there have as yet been no reports of simple alkyl sulfide complexes of CuSCN. The only related structure we uncovered was that of $(CuSCN)_2$(1,10-dithia-18-crown-6) [7]. In this complex the bis-sulfide ligand bridges $[Cu_2(SCN)_2]_\infty$ ladders, forming a sheet network. Only the sulfur atoms in the crown ether/thioether molecule coordinate to Cu(I); the harder oxygen atoms fail to interact with the soft Cu(I). Herein we present the synthesis of five new CuSCN-L compounds, containing the aliphatic sulfides L = Me_2S, Et_2S, $Pr^i{}_2S$, and THT. Four new crystal structures, falling in CuSCN chain and ladder categories, were solved and are discussed.

2. Experimental

2.1. Materials and methods

All reagents were purchased from Aldrich or Acros and used without purification. Commercial CuSCN (Aldrich) was shown by FTIR to consist solely of the α-phase [8]. IR spectra were collected on a Shimadzu IRTracer-100 instrument using a diamond ATR probe (spectra shown in Supporting Information). Analyses for C, H, and N proved impossible for the compounds described herein due to high ligand lability. Atomic absorption (AAS) analyses for Cu were carried out using a Perkin–Elmer AAnalyst 700 as previously described [9]. Thermogravimetric analyses (TGA) were conducted using a TA Instruments Q500 in the dynamic (variable temp.) mode with a maximum heating rate of 50 °C/min. to 800 °C under 50 mL/min. N_2 flow.

2.2. Syntheses

2.2.1. *$\{[Cu(SCN)(Me_2S)_2]\}_n$*, ***1a***

CuSCN (131 mg, 1.07 mmol) was dissolved in 480 μL of neat Me_2S in a vial. The resulting brown solution was placed in a freezer for 3 d. The colorless crystals that formed were collected by siphoning excess ligand from the vial. The crystals were washed

* Corresponding author.

http://dx.doi.org/10.1016/j.poly.2016.05.029
0277-5387/

with pentane and air-dried for no more than 5 min. Yield: 82 mg, 38.9%. Samples were immediately analyzed via TGA, IR, and AAS. IR (cm^{-1}): 2920 (weak), 2098 (v strong), 1419, 1029, 979, 771, 682. *Anal.* Calc. for $C_5H_{12}NCuS_3$: Cu, 25.8. Found: Cu, 25.2%. Due to sample instability, CHN analysis was not possible. TGA calcd for (CuSCN)(Me_2S): 74.7%. Found: 70.2% (20–50 °C). Calcd for CuSCN: 49.4%. Found: 53.6% (50–130 °C).

2.2.2. {[(CuSCN)(Me_2S)]}$_n$, **1b**

CuSCN (271 mg, 2.23 mmol) was dissolved in 1.5 mL of neat Me_2S. The resulting suspension was stirred at room temperature for 1 h in a sealed vial, with the solid dissolving completely into the ligand after only a few minutes. The product was precipitated with addition of pentane. The resulting white solid was collected via filtration, and washed with pentane. Because of the ready loss of sulfide, the product was dried for no more than 5 min. prior to storage in a freezer (271 mg, 51.3% yield). Samples were immediately analyzed via TGA, IR, and AAS. IR (cm^{-1}): 2117 (v strong), 1415, 1037, 975, 759. *Anal.* Calc. for $C_3H_6NCuS_2$: Cu, 34.6. Found: Cu, 35.1%. Due to sample instability, CHN analysis was not possible. TGA calculated for CuSCN: 66.1%. Found: 67.1% (35–120 °C).

2.2.3. {[Cu(SCN)(Et_2S)]}$_n$, **2**

CuSCN (96 mg, 0.798 mmol) was dissolved in 2 mL of neat Et_2S in a vial. The solid dissolved within 20 min. with stirring. The solution was stirred for 3 d. Precipitation with ethyl ether resulted in a white powder, which was isolated by filtration and washed with ether. The product was dried for no more than 5 min. due to ready loss of ligand (103 mg, 61.6%). Due to sample instability, CHN analysis was not possible. IR (cm^{-1}): 2970 (weak), 2169 (v strong), 1446, 1377, 1259, 974, 746. *Anal.* Calc. for $C_5H_{10}CuNS_2$: Cu, 30.0. Found: Cu, 32.5%. TGA calculated for CuSCN: 58.4%. Found: 61.6% (45–95 °C).

2.2.4. {[Cu(SCN)(Pr^i_2S)]}$_n$, **3**

The procedure for **2** was followed, using 85 mg (0.699 mmol) CuSCN and 2 mL of neat Pr^i_2S. The solid did not dissolve completely. The suspension was stirred for 3 d. A white powder was collected via filtration and washed with ethyl ether (110 mg, 65.6%). IR (cm^{-1}): 2974 (weak), 2924 (weak), 2866 (weak), 2924 (weak), 2866 (weak), 2110 (strong), 1442, 1381, 1365, 1238, 1153, 1045, 929, 906, 883, 860, 748. *Anal.* Calc. for $C_7H_{14}CuNS_2$: Cu, 26.5. Found: Cu, 26.9%. Due to sample instability, CHN analysis was not possible. TGA calculated for CuSCN: 50.7%. Found: 54.8% (40–75 °C).

2.2.5. {[Cu(SCN)($THT)_2$]}$_n$, **4**

The procedure for **2** was followed, using 91 mg (0.748 mmol) CuSCN and 2 mL of neat THT. The solid did not dissolve completely. The suspension was stirred for 3 d. A white powder was collected via filtration and washed with ethyl ether (186 mg, 83.4%). IR (cm^{-1}): 2951, 2125 (strong), 1435, 1253, 883, 756, 671. *Anal.* Calc. for $C_9H_{16}CuNS_3$: Cu, 21.3. Found: Cu, 21.6%. Due to sample instability, CHN analysis was not possible. TGA calcd for (CuSCN)(THT): 70.4%, Found: 72.8 (31–50 °C). Calcd for CuSCN: 40.0%. Found: 43.3% (60–95 °C).

2.3. Crystallizations

Single crystals were grown using several techniques. Once removed from mother liquor, all crystals were immediately placed into Paratone N oil and then mounted under a stream of dry air at 100 K. Crystals of **1a** were grown as described above, resulting in colorless blocks. For **2**, 80 mg of CuSCN were stirred in 2 mL of Et_2S for 1 h. The vial was then left uncapped and undisturbed in a fume hood. Overnight evaporation of excess Et_2S left colorless blades of **2**. For **3** and **4**, 119 mg of CuSCN were stirred with 4 mL of neat THT, and 117 mg of CuSCN were stirred with 4 mL of neat Pr^i_2S in sealed vials under Ar in an oil bath at 70 °C for 3 d. CuSCN dissolved completely in THT in this procedure. The vial was allowed to cool to room temp before being placed in a freezer. Colorless plates of **4** grew over 3 d. Although the Pr^i_2S compound never fully dissolved in the neat ligand, long colorless needles of **3** suitable for diffraction grew as the vial was left to cool at room temp.

2.4. X-ray data collection, structure solutions and refinements

All X-ray measurements were made using graphite-monochromated Cu Kα radiation on a Bruker-AXS three-circle diffractometer, equipped with a SMART Apex II CCD detector. Crystals of **2** and **4** underwent destructive phase changes at reduced temperatures, even as high as 250 K. Data for **2** and **4** were collected at room temperature (298 K). Data for **1a** and **3** were collected at 100 K. Initial space group determination was based on a matrix consisting of 120 frames. The data were corrected for Lorentz and polarization [10] effects and absorption using SADABS [11]. The structures were solved using intrinsic phasing methods. Structure solution, refinement and the calculation of derived results were performed using the SHELXTL [12] package of software and ShelXle [13]. Non-hydrogen atoms were refined anisotropically. Hydrogen atoms were placed in theoretical positions.

Powder diffraction analysis was carried out on the instrument described above. Samples were rapidly ground and prepared as mulls using Paratone N oil. Four 180 s frames were collected, covering 8–100° 2θ. Frames were merged using the SMART Apex II software [14] and were further processed using DIFFRAC.EVA software [15].

3. Results and discussion

3.1. Synthesis and characterization

Copper(I) thiocyanate complexes with dialkyl sulfide ligands were generated easily via dissolution or suspension of CuSCN in neat sulfide ligand. The off-white CuSCN dissolved completely in Me_2S and Et_2S after only a few minutes of stirring. A white ligated product was readily precipitated from the neat sulfide solution via addition of pentane or ethyl ether. Although CuSCN was not fully soluble in Pr^i_2S or THT at room temperature, stirring of the two-phase mixtures over several days enabled complete conversion to the white sulfide products. Reaction of CuSCN was found to afford two different products from neat Me_2S solution, depending on the conditions of product isolation. Colorless crystals grown by cooling highly concentrated solutions of CuSCN in Me_2S were found to be have 1:2 stoichiometry: (CuSCN)(Me_2S)$_2$, **1a**. This result was confirmed via both X-ray diffraction and TGA. A white powder obtained by pentane precipitation of the solid from the CuSCN/Me_2S solution analyzed as a 1:1 compound: (CuSCN)(Me_2S), **1b**, by thermogravimetric analysis (TGA) and atomic absorption analysis. As shown in Fig. 1, the Me_2S compounds produced distinct X-ray powder diffraction traces. Each of the other sulfides produced only a single product phase when reacted with CuSCN: {[Cu(SCN)(Et_2S)]}$_n$, **2**, {[Cu(SCN)(Pr^i_2S)]}$_n$, **3**, and {[Cu(SCN)(THT)$_2$]}$_n$, **4**.

None of the five compounds prepared herein was thermally stable. Instead, each compound steadily lost ligand at ambient temperature over the course of hours. This was apparent upon examination of TGA data collected on samples after relatively short and longer drying times. Thermal decomposition is expected to cause quantitative removal of organic ligand from CuSCN-L

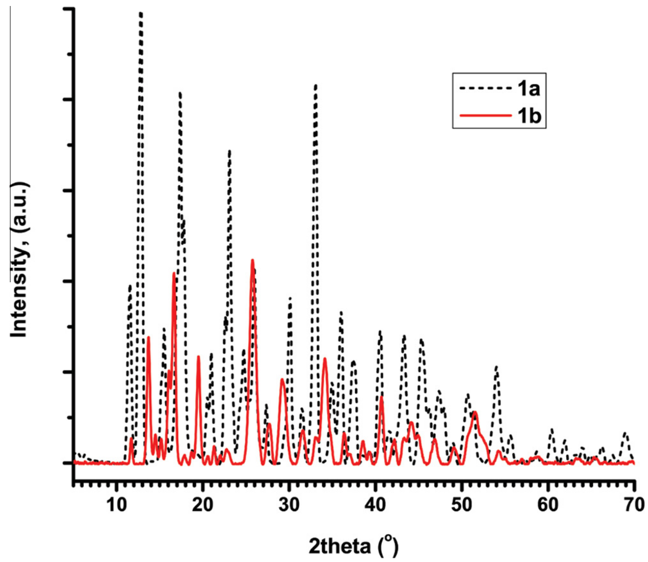

Fig. 1. Powder X-ray diffraction comparison of complexes **1a** and **1b**.

complexes. The complexes air-dried for no more than five minutes showed ligand loss plateaus by TGA that corresponded to the theoretical mass of CuSCN (see Fig. S1). The sulfide ligands were removed between ambient temperature and 135 °C, leaving CuSCN, which itself decomposed around 400–450 °C. However, samples dried for longer periods or under vacuum showed plateaus after ligand loss that indicated elevated CuSCN content. The alkyl sulfide-CuSCN compounds proved to be stable in sealed vials at −5 °C for a period of days to weeks. The instability the alkyl sulfide products reported herein are likely to be the result of excess electron donation at the Cu(I) center.

3.2. Description of X-ray structures

A total of four crystal structures were solved during the course of this study. The resulting structures fall into two recognized categories: 1-D chains and 1-D ladders. All of the alkyl sulfide compounds were found to behave as monodentate capping ligands, precluding the formation of multidimensional networks. This was a surprising finding given the propensity of alkyl sulfide ligands to bridge in complexes of CuCl, CuBr, CuI, and CuCN [2]. Crystallographic data are summarized in Table 1. Selected bond lengths and angles are given in Table S1.

Compound **1a** crystallized as colorless blocks that solved in centrosymmetric monoclinic space group $P2_1/c$. A chain diagram is shown in Fig. 2. The structure consists of a 1-D CuSCN chain with the four-coordinate Cu centers capped by pairs of Me_2S ligands. The CuSCN chain propagates along the crystallographic *c*-axis. Both Cu–S bonds associated with the sulfide molecules (Cu–S2 = 2.3456(5), Cu–S3 = 2.2869(4) Å) are shorter than that of the thiocyanate (Cu–S1 = 2.3783(6) Å). The chain has a zigzag angle N1–Cu1–S1 of 106.73(5)°. This is the smallest of the roughly tetrahedral angles about Cu, which range from 106.73(5)° to 117.24(5)°. The single independent CuSCN unit lies in two positions that are slightly displaced from one another, such that a Cu1···Cu1···Cu1 angle of 173.64° and a S1···Cu1···Cu1···S1 dihedral angle of 27.06° are seen. There are no apparent inter-chain interactions.

Compound **2** crystallized as colorless blades that solved in the centrosymmetric monoclinic space group $P2_1/n$. The asymmetric unit consists of Cu(SCN)(Et_2S). A structure diagram is shown in Fig. 3. Crystals of this compound underwent a destructive phase change upon modest reduction in temperature, necessitating data collection at 298 K. Even the ambient temperature structure retained relatively poor crystallographic ordering. The disordered Et_2S ligand was modeled over two positions, and still shows rather larger thermal ellipsoids (see Supporting Information). The network in **2** consists of CuSCN ladders capped by Et_2S ligands. The ladders are formed by the crosslinking of antiparallel CuSCN chains by μ_3-S. The sulfur atoms of the thiocyanate groups bridge between pairs of Cu atoms, resulting in alternating, edge-sharing Cu_2S_2 and $Cu_2(SCN)_2$ dimers. The ladders propagate along the crystallographic *a*-axis. A single diethyl sulfide ligand completes the roughly tetrahedral coordination sphere around copper (angles = 103.16(8)–121.80(12)°). In **2**, the distance between the Cu atoms across the rhomboid Cu_2S_2 dimer is 2.8893(7) Å, falling just outside the van der Waals radius sum for copper (2.8 Å). This short distance results in a relatively small Cu–S–Cu angle of 72.74(3)°. Distances between Cu and thiocyanate S (Cu–S = 2.368(1), 2.500(1) Å) are slightly longer than those between Cu and S of the aliphatic ligand (Cu–S2A = 2.227(5), Cu–S2B = 2.294(9) Å). Adjacent ladders are rotated by 90° with respect to one another, and there are no significant interactions between the ladders.

Compound **3** crystallized as thin colorless needles that solved in the centrosymmetric monoclinic space group $P2_1/n$. The asymmetric

Table 1
Crystal and structure refinement data.

Complex	**1a**	**2**	**3**	**4**
CCDC deposit No.	1460762	1460764	1460765	1460763
Color and habit	colorless block	colorless prism	colorless prism	colorless plate
Size (mm)	0.49 × 0.42 × 0.26	0.45 × 0.14 × 0.11	0.63 × 0.10 × 0.08	0.38 × 0.21 × 0.06
Formula	$C_5H_{12}CuNS_3$	$C_5H_{10}CuNS_2$	$C_7H_{14}CuNS_2$	$C_9H_{16}CuNS_3$
Formula weight	245.88	211.80	239.85	297.95
Space group	$P2_1/c$ (#14)	$P2_1/n$ (#14)	$P2_1/n$ (#14)	$P2_1$ (#4)
a (Å)	7.39230(10)	5.82340(10)	5.92320(10)	5.8965(2)
b (Å)	13.0297(3)	9.6077(2)	10.9226(2)	9.3775(3)
c (Å)	11.2206(2)	16.2675(4)	15.9989(3)	11.7823(3)
β (°)	108.7360(10)	96.4230(10)	91.4730(10)	98.004(2)
V (Å^3)	1023.49(3)	904.45(3)	1034.73(3)	645.15(3)
Z	4	4	4	2
ρ_{calc} (g cm^{-3})	1.596	1.555	1.540	1.534
F(000)	504	432	496	308
μ(Cu Kα) (mm^{-1})	8.211	7.093	6.271	6.626
T (K)	100(2)	296(2)	100(2)	296(2)
Residuals:[a] *R*; R_w	0.0232; 0.0581	0.0327; 0.0936	0.0228; 0.0589	0.0294; 0.0737
Goodness of fit (GOF) on F^2	1.209	1.038	0.997	1.103
Flack	–	–	–	0.03(4)

[a] $R = R_1 = \sum||F_o| - |F_c||/\sum|F_o|$ for observed data only. $R_w = wR_2 = \{\sum[w(F_o{}^2 - F_c{}^2)^2]/\sum[w(F_o{}^2)^2]\}^{1/2}$ for all data.

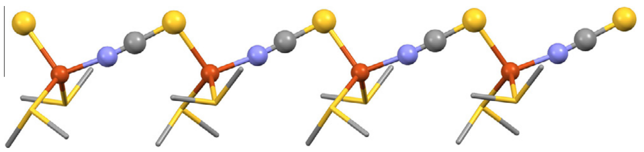

Fig. 2. The chain structure of **1a** viewed along *b*-axis CuSCN atoms shown as ball and stick, and Me_2S atoms as wireframe. Hydrogen atoms are omitted. Color scheme for all X-ray figures: orange = Cu, yellow = S, grey = C, blue = N. Selected bond lengths (Å) and angles (°): Cu–SCN = 2.3784(5), Cu–NCS = 1.9493(17), Cu–SR_2 = 2.2868(5), 2.3456(5), Cu–S–C = 96.41(7), C–N–Cu = 170.51(16). (Color online.)

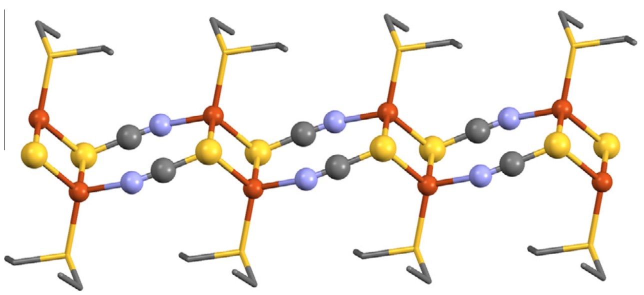

Fig. 3. The ladder structure of **2** viewed along *c*-axis. CuSCN atoms shown as ball and stick, and Et_2S atoms as wireframe. Hydrogen atoms and disordered ligand positions are omitted. Selected bond lengths (Å) and angles (°): Cu–SCN = 2.3684 (11), 2.5004(10), Cu–NCS = 1.961(3), Cu–SR_2 = 2.227(6), Cu···Cu = 2.8895(10), Cu–S–C = 95.30(11), 106.60(12), C–N–Cu = 161.2(2), Cu–S–Cu = 72.75(3).

unit consists of Cu(SCN)($Pr^i{}_2S$). A structural diagram is shown in Fig. 4. This compound displays the same ladder networking as was seen with **2**. Unlike **2**, the crystal did not undergo a destructive phase change at reduced temperatures, and the ligand molecules were not disordered. Some important structural differences between **2** and **3** are apparent when examining the Cu_2S_2 dimers. The ladders in **3**, which propagate along the *a*-axis are all aligned, unlike those in **2**. In **3**, the dimer Cu···Cu = 3.1662(5) Å, with a corresponding dimer Cu–S–Cu angle of 81.08(2)°. This trend of increasing Cu–S–Cu angle with increasing Cu···Cu has been noted in other CuSCN ladder compounds and in $(CuI)_2$Qox, which contains both long and short Cu···Cu [6,9,16]. As was the case in **1a** and **2**, bond distances between the copper and thiocyanate sulfur atoms (2.4816(6) and 2.3883(6) Å) are slightly longer than that for the sulfide ligand (2.2740(5) Å). There are no interactions between adjacent ladders.

Compound **4** crystallized as thin, colorless and transparent plates, solving in the non-centrosymmetric monoclinic space group $P2_1$. As was the case with **2**, the crystals of **4** underwent a destructive phase just below ambient temperature, and so data were collected at 298 K. The complex also showed ligand disorder

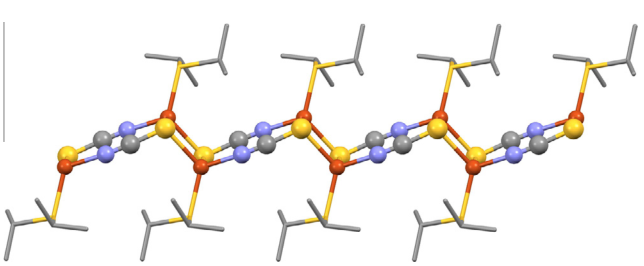

Fig. 4. The ladder structure of **3** viewed along *c*-axis. CuSCN atoms shown as ball and stick, and $Pr^i{}_2S$ atoms as wireframe. Hydrogen atoms are omitted. Selected bond lengths (Å) and angles (°): Cu–SCN = 2.3883(5), 2.4816(5), Cu–NCS = 1.9629 (16), Cu–SR_2 = 2.2739(5), Cu···Cu = 3.1662(6), Cu–S–C = 97.08(7), 107.43(7), C–N–Cu = 160.64(15), Cu–S–Cu = 81.084(17).

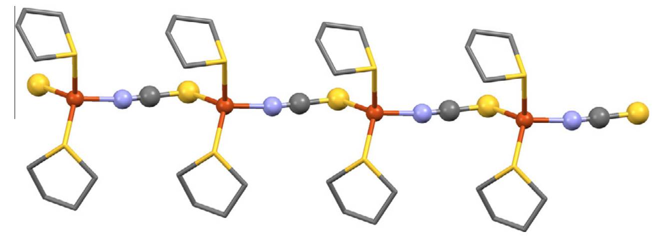

Fig. 5. The chain structure of **4** viewed along *b*-axis. CuSCN atoms shown as ball and stick, and THT atoms as wireframe. Hydrogen atoms and disordered ligand positions are omitted. Selected bond lengths (Å) and angles (°): Cu–SCN = 2.3438 (15), Cu–NCS = 1.967(5), Cu–SR_2 = 2.187(19), 2.400(17), Cu–S–C = 105.07(18), C–N–Cu = 173.4(4).

(see Supporting Information). In this case there are two THT ligands, both of which were modeled over two disordered positions. Like **1a**, the structure of **4** consists of a 1-D CuSCN chain with four-coordinate Cu atoms capped by pairs of THT ligands. The CuSCN chain propagates along the *a*-axis. A chain diagram is shown in Fig. 5. The zigzag angle, N1–Cu1–S1, is 110.06(15)°, and all angles around Cu are fairly close to tetrahedral: 103.5(3)–117.7(6)°. Unlike **1a**, the thiocyanate Cu–S (2.344(2) Å), falls within the range of the Cu–S_{THT} distances: Cu–S2A = 2.40(2), Cu–S2B = 2.35(2) Cu–S3A = 2.19(2), Cu–S3B = 2.366(6) Å. Once again, no significant interactions between chains are noted.

4. Conclusions

We have reported the first alkyl monosulfide complexes of copper(I) thiocyanate. Five compounds were prepared by the reaction of CuSCN in neat Me_2S, Et_2S, $Pr^i{}_2S$, and tetrahydrothiophene (THT). In the former case $\{[Cu(SCN)(Me_2S)_2]\}_n$ (**1a**) forms upon cooling a solution of CuSCN in Me_2S, while $\{[(CuSCN)(Me_2S)]\}_n$ (**1b**) is formed by rapid precipitation from the solution. Only $\{[Cu(SCN)(Et_2S)]\}_n$ (**2**) can be realized from a solution of CuSCN in Et_2S. Sulfide compounds $\{[Cu(SCN)(Pr^i{}_2S)]\}_n$ (**3**) and $\{[Cu(SCN)(THT)_2]\}_n$ (**4**) are formed from suspensions of CuSCN in the ligand. All compounds are thermally unstable, losing alkyl sulfide ligand over a course of hours at room temperature. None of the complexes show bridging through the sulfide ligand. Compounds **1a** and **4** consist of zigzag CuSCN chains decorated with pairs of monodentate sulfide ligands. Compounds **2** and **3** consist of ladders of alternating and edge sharing Cu_2S_2 and $(CuSCN)_2$ rungs. In both cases a monodentate sulfide ligand fills out the tetrahedral copper coordination sphere. The sulfide compounds of CuSCN appear to be far less stable than those of the copper(I) halides and cyanide. This instability of CuSCN-SR_2 appears to be connected with the failure to promote network formation.

Acknowledgement

We are indebted to NSF (CHE-0443345) and the College of William and Mary for the purchase of the X-ray equipment.

Appendix A. Supplementary data

CCDC 1460762–1460765 contains the supplementary crystallographic data for **1a** and **2**–**4**. These data can be obtained free of charge via http://www.ccdc.cam.ac.uk/conts/retrieving.html, or from the Cambridge Crystallographic Data Centre, 12 Union Road, Cambridge CB2 1EZ, UK; fax: (+44) 1223 336 033; or e-mail: deposit@ccdc.cam.ac.uk. Supplementary data associated with this article can be found, in the online version, at http://dx.doi.org/10.1016/j.poly.2016.05.029.

References

[1] (a) H.O. House, C.-Y. Chu, J.M. Wilkins, J.J. Umen, J. Org. Chem. 40 (1975) 1460;
(b) B.H. Lipshutz, S. Whitney, J.A. Kozlowski, C.M. Breneman, Tetrahedron Lett. 27 (1986) 4273;
(c) S.H. Bertz, C.P. Gibson, G. Dabbagh, Organometallics 7 (1988) 227.

[2] (a) B. Lenders, D.M. Grove, W.J.J. Smeets, P. van der Sluis, A.L. Spek, G. van Koten, Organometallics 10 (1991) 786;
(a) B. Lenders, D.M. Grove, W.J.J. Smeets, P. van der Sluis, A.L. Spek, G. van Koten, Organometallics 10 (1991) 786;
(b) H. Maelger, F. Olbrich, J. Kopf, D. Abein, E. Weiss, Z. Naturforsch. 47b (1992) 1276;
(c) J. Zhou, G.-Q. Bian, J. Dai, Y. Zhang, Q.-Y. Zhu, W. Lu, Inorg. Chem. 45 (2006) 8486;
M. Heller, W.S. Sheldrick, Z. Anorg. Allg. Chem. 630 (2004) 1869;
(e) M.D. Dembo, L.E. Dunaway, J.S. Jones, E.A. Lepekhina, S.M. McCullough, J.L. Ming, X. Li, F. Baril-Robert, H.H. Patterson, C.A. Bayse, R.D. Pike, Inorg. Chim. Acta 364 (2010) 102;
(f) K.M. Henline, C. Wang, R.D. Pike, J.C. Ahern, B. Sousa, H.H. Patterson, A.T. Kerr, C.L. Cahill, Cryst. Growth Des. 14 (2014) 1449;
(g) P.D. Harvey, M. Knorr, J. Clust. Sci. 26 (2015) 411;
(h) M. Knorr, A. Bonnot, A. Lapprand, A. Khatyr, C. Strohmann, M.M. Kubicki, Y. Rousselin, P.D. Harvey, Inorg. Chem. 54 (2015) 4076;
(i) A. Bonnot, M. Knorr, F. Guyon, M.M. Kubicki, Y. Rousselin, C. Strohmann, D. Fortin, P.D. Harvey, Cryst. Growth Des. 16 (2016) 774.

[3] (a) D. Li, T. Wu, X.-P. Zhou, R. Zhou, X.-C. Huang, Angew. Chem., Int. Ed. 44 (2005) 4175;
(b) J. Wang, Y.-H. Zhang, H.-X. Li, Z.-J. Lin, M.-L. Tong, Cryst. Growth Des. 7 (2007) 2352;
(c) Z.-M. Hao, J. Wang, X.-M. Zhang, CrystEngComm 12 (2010) 1103.

[4] (a) F.B. Stocker, M.A. Troester, D. Britton, Inorg. Chem. 35 (1996) 3145;
(b) F.B. Stocker, M.A. Troester, Inorg. Chem. 35 (1996) 3154;
(c) F. Grifasi, M.R. Chierotti, C. Garino, R. Gobetto, E. Priola, E. Diana, F. Turci, Cryst. Growth Des. 15 (2015) 2929.

[5] (a) O.N. Kataeva, D.B. Krivolapov, A.T. Gubaidullin, I.A. Litvinov, L.I. Kursheva, S.A. Katsyuba, J. Mol. Struct. 554 (2000) 127;
(b) P.W.R. Corfield, Acta Crystallogr., Sect. E 70 (2014) 281.

[6] G. Ayala, T.A. Tronic, R.D. Pike, Polyhedron 115 (2016) 257.

[7] T. Röttgers, W.S. Sheldrick, Z. Anorg. Allg. Chem. 627 (2001) 1976.

[8] G.A. Bowmaker, J.V. Hanna, Z. Naturforsch. B 64 (2009) 1478.

[9] P.M. Graham, R.D. Pike, Inorg. Chem. 39 (2000) 5121.

[10] SAINT PLUS, Bruker Analytical X-ray Systems, Madison, WI, 2001.

[11] SADABS, Bruker Analytical X-ray Systems, Madison, WI, 2001.

[12] G.M. Sheldrick, Acta Crystallogr., Sect. A. 64 (2008) 112.

[13] C.B. Hubschle, G.M. Sheldrick, B. Dittick, J. Appl. Crystallogr. 44 (2011) 1281.

[14] SMART Apex II, Data Collection Software, version 2.1, Bruker AXS Inc., Madison, WI, 2005.

[15] DIFFRAC.EVA, version 3.1, Bruker AXS Inc., Madison, WI, 2013.

[16] (a) Q. Wang, G. Guo, T.C.W. Mak, Chem. Commun. (1999) 1849;
(b) Z. Hao, X. Zhang, Cryst. Growth Des. 7 (2007) 64;
(c) R.J. Trovitch, R.S. Rarig, J.A. Zubieta, R.L. LaDuca, Acta Crystallogr., Sect. E. 63 (2007) m339;
(d) C. Näther, M. Wriedt, Dalton Trans. 46 (2009) 10125;
(e) R. Peng, D. Li, T. Wu, X. Zhou, S.W. Ng, Inorg. Chem. 45 (2006) 4035;
(f) S. Liang, M. Li, M. Shao, X. He, J. Mol. Struct. 875 (2008) 17;
(g) W.R. Knapp, J.G. Thomas, D.P. Martin, M.A. Braverman, R.J. Trovitch, R.L. LaDuca, Z. Anorg. Allg. Chem. 875 (2007) 575.